

Efficiency of H₂O₂-treated eucalyptus biochar on the removal of Cu(II), Cd(II) and Ni(II) from aqueous solution

Elias Costa de Souza¹, Alexandre Santos Pimenta¹, Alfredo José Ferreira da Silva², Renata Martins Braga¹, Tatiane Kelly Barbosa de Azevedo¹, Pedro Nicó de Medeiros Neto³

¹ Universidade Federal do Rio Grande do Norte, Programa de Pós-Graduação em Ciências Florestais, Unidade Acadêmica Especializada em Ciências Agrárias, Macaíba, RN, Brasil. E-mail: eliasrem@hotmail.com; alexandre_spimenta@hotmail.com; renatabraga.r@gmail.com; tatianekellyengenhaira@hotmail.com

² Universidade Federal do Rio Grande do Norte, Programa de Pós-Graduação em Engenharia Química, Núcleo de Ensino e Pesquisa em Petróleo e Gás, Natal, RN, Brasil. E-mail: alfredo@nupeg.ufrn.br

³ Universidade Federal de Campina Grande, Programa de Pós-Graduação em Ciências Florestais, Patos, PB, Brasil. E-mail: pedroflorestal@gmail.com

ABSTRACT: The present work had the goal to produce H₂O₂-treated biochar from eucalyptus wood and testing its efficiency in the removal of heavy metals from aqueous solutions. Oxidizing treatment was performed by reacting biochar with H₂O₂ (10% m/m) during 4 hours at pH 8.0 and 80 °C. Fresh and H₂O₂-treated biochar samples were characterized by thermogravimetry and elemental analysis. Point of zero charge and specific surface area were determined. Adsorption kinetics tests with Cu were carried out and Langmuir and Freundlich isotherms were adjusted. Adsorption tests were conducted with a mixture of Cu, Ni and Cd cations in aqueous solution. The best adsorption capacity was achieved in acid pH. H₂O₂-treated biochar had adsorption capacity of 170.41 mg L⁻¹ for Cu alone and 305.35 mg L⁻¹ for the mixture of metals. Adsorption was best predicted by the Langmuir isotherm (R² = 0.9976). Despite the significant decrease in the specific surface area, the H₂O₂-treated biochar showed better performance in the adsorption of heavy metals compared to the original biochar, especially in the presence of more than one metallic cation.

Key words: adsorption of heavy metals; biochar; kinetics of adsorption; oxidation with hydrogen peroxide

Eficiência do biochar de eucalipto tratado com H₂O₂ na remoção de Cu (II), Cd (II) e Ni (II) de soluções aquosas

RESUMO: O presente trabalho teve como objetivo produzir carvão tratado com H₂O₂ a partir de madeira de eucalipto e testar sua eficiência na remoção de metais pesados de soluções aquosas. O tratamento oxidante foi realizado por reação do carvão com H₂O₂ (10% m/m) durante 4 horas com temperatura de 80 °C e pH 8,0. Amostras de biochar com e sem tratamento com H₂O₂ foram caracterizadas por termogravimetria e análise elementar. O ponto de carga zero e a área superficial específica foram determinadas. Foram realizados testes de cinética de adsorção com Cu (II) e ajustadas as isotermas de Langmuir e Freundlich. Os testes de adsorção foram realizados com uma mistura de cátions Cu (II), Ni (II) e Cd (II) em solução aquosa. A melhor capacidade de adsorção foi alcançada no pH ácido. O carvão tratado com H₂O₂ teve capacidade de adsorção de 170,41 mg L⁻¹ somente para Cu e 305,35 mg L⁻¹ para a mistura de metais. A adsorção foi melhor estimada pela isoterma de Langmuir (R² = 0,9976). Apesar da redução significativa na área superficial específica, o carvão tratado com H₂O₂ apresentou melhor desempenho na adsorção de metais pesados em comparação com o carvão original, especialmente na presença de mais de um cátion metálico.

Palavras-chave: adsorção de metais pesados; biocarvão; cinéticas de absorção; oxidação com peróxido de hidrogênio

Introduction

Biochar, a byproduct resultant from pyrolysis of several types of lignocellulosic raw materials, stands out as an efficient amendment for soil quality improvement, usually showing positive effects on its physical and chemical properties besides enhancing agricultural production (Glaser et al., 2002; Verheijen et al., 2010; Novotny et al., 2015; Zhang et al., 2018). After addition to soil, biochar undergoes a natural process of oxidation or aging where its chemical structure is oxidized to molecular benzene polycarboxylic acids (Mia et al., 2017; Aller et al., 2017). As result of natural oxidation, the adsorption capacity of biochar and its interaction with ions increases significantly, behavior explained by the higher number of oxygenated functional groups in the material's chemical structure (Glaser et al., 2002). However, the oxidation process can be artificially accelerated by several methods, including drying or wetting or methods encompassing the reaction of biochar with nitric acid, hydrogen peroxide, potassium permanganate and some other chemical agents (Glaser et al., 2002; Liu & Zhang, 2009; Frišták et al., 2015; Mia et al., 2017). Therefore, as consequence of the increase in the amount of functional groups in the structure with oxidation, the cation exchange capacity of biochar increases and the carbon concentration decreases (Cheng et al., 2008; Cheng & Lehmann, 2009; Nguyen et al., 2010; Peng et al., 2011).

Activated charcoals (AC), considered as universal biosorbents, are efficient agents to remove heavy metals from aqueous media, as well as for adsorption of gases and other kinds of contaminants. Despite its undeniable efficiency, most commercial AC are produced by chemical activation processes that, usually are expensive and involve high temperatures (Miao et al., 2013; Tiryaki et al., 2014; Köseoğlu & Akmil-Başar, 2015). Therefore, research into alternative and cheaper biosorbents is important to substitute or complement ACs use as well as reduce costs of the removal of heavy metals from soils, wastewaters and other liquid effluents. Regarding heavy-metal contaminated soils, Lahori et al. (2017) published a comprehensive review describing in detail how efficient biochar can be in removing those pollutants and reducing their availability to crops. Other authors have reported the use of chemically treated biochar for heavy metal adsorption. They verified that the oxidation process significantly increased the adsorption capacity, mainly as a function of the increase in the number of functional groups in the biochar structure (Wang et al., 2015; Frišták et al., 2015; Zuo et al., 2016; Xu et al., 2018; Wang & Liu 2018).

However, to enable large-scale production of biosorbents, the raw materials have to be available in large amounts throughout the year, besides being cheap and easy to handle. Eucalyptus biochar meets all those conditions. In Brazil, there are about 5.6 million hectares of forests planted with eucalyptus, being 1.1 million hectares applied entirely to charcoal making, industrial activity which reached 4.5 million metric tons in 2016 (BTI, 2017). Nearly 85% of that charcoal was consumed in metallurgy, specifically by of pig iron, steel, iron alloys and

silicon industries, the well-known Brazilian green metallurgy. In the last 10 years, metallurgy companies have been making efforts to improve the pyrolysis performance and develop new products to add value to the charcoal productive chain. In this respect, eucalyptus biochar is an option to considered and investigated to possibly be used as a decontaminant to remove heavy metals from soil and liquid effluents. This way chemical oxidation seems to be an obvious alternative tool to improve the adsorption capacity of biochar turning it into a high-quality and ready-to-use product.

The present work had the general objective of evaluating the efficiency of eucalyptus biochar before and after oxidizing treatment with hydrogen peroxide on the removal of heavy metals from aqueous solutions. As a more specific goal, the effects of pH on the heavy metal's adsorption and as well its kinetics were assessed.

Materials and Methods

Biochar preparation

The eucalyptus wood (a hybrid of *Eucalyptus urophylla* x *Eucalyptus grandis*, in Brazil called as *Eucalyptus urograndis*) was collected from clonally propagated trees located in the Agricultural Sciences Unit of Rio Grande do Norte Federal University, Macaíba, Rio Grande do Norte (05° 51' 30" S and 35° 21' 14" W). Procedures for logs collection and wood sampling were carried out by the method recommended by Santos et al. (2013). Wood samples consisted of 3.0 cm thickness disks divided into four wedges each. Wood wedges were oven dried for 48 hours at 103 ± 1 °C until reaching constant weight. Then batches of about 500 g of wood wedges were placed in a metallic container and carbonized in a muffle furnace at a heating rate of 0.94 °C min⁻¹ until reaching 450 °C, equivalent to a run time of 8 hours. Ten charring runs were performed, holding the final temperature for 30 min.

Biochar H₂O₂-treatment

The experimental condition for biochar oxidation with hydrogen peroxide was optimized in a previous work by using a factorial experiment carried out by Oliveira (2017), involving two reaction times (2 and 4 hours) and two concentrations of oxidant reagent (10 and 20% m/m). Oxidation reaction of biochar was accomplished as follows. In a 1,000 mL glass reactor, 40 g of ground biochar (granulometry < 100 mesh) was placed in a 1,000 mL glass reactor along with 250 g of a hydrogen peroxide solution (10% m/m). The solution pH was adjusted to 8.0 by using a solution of NaOH (50% m/m). The mixture was maintained at 80 °C during 4 hours under continuous magnetic stirring. After the reaction was concluded, 600 mL of deionized water was added to the mixture and the solution was filtered. H₂O₂-treated biochar was oven dried at 60 °C for 24 hours and stored for further analyses.

Instrumental characterization of samples

Both fresh and H₂O₂-treated biochar samples were analyzed with a Netzsch TG-209 F3 thermogravimetric analyzer. The

runs were carried out under oxygen atmosphere with heating rate of 5 °C min⁻¹, from room temperature until 650 °C, with a 30 min interruption at 105 °C to measure the moisture content (weight loss percentage). Additionally, a parameter called thermogravimetric index (TGI) was calculated by the method proposed by Benites et al. (2005) and Trompowsky et al. (2005). According those authors, TGI is defined as the ratio between the areas under thermogravimetric curves corresponding, respectively, to the weight loss occurring in the range of 105 to 350 °C and the weight loss occurring from 350 to 650 °C.

Samples were characterized by scanning electron microscopy with a Tescan Vega 3 microscope. Elemental analysis of the samples was carried out with a Perkin-Elmer 2400 CHNS/O Series II elemental analyzer system with two replicates per sample. The specific surface area (m² g⁻¹) of fresh and H₂O₂-treated biochar was measured by using the BET multipoint method with a Quantachrome Nova 4200e surface analyzer.

Point of zero charge (PZC) was determined by using a NanoBrook 90Plus zeta potential analyzer (Brookhaven Instruments) with 0.5 g of each biosorbent (fresh and H₂O₂-treated biochar) in 500 mL of deionized water, varying pH from 2 to 6. For each sample, two replicates were carried out. For the adjustment of pH, a 0.1 mol L⁻¹ NaOH solution was used. Before pH determination, all the aqueous suspensions were maintained under stirring for 24 h.

Adsorption kinetics tests

For adsorption kinetic tests, 0.5 g of both biochar samples was added to 50 mL of a Cu²⁺ solution (copper sulfate pentahydrate – Merck™) with a concentration of 50 mg L⁻¹. The solutions were maintained under constant stirring of 150 rpm. At intervals previously determined (0.5, 1, 5, 10, 15, 20, 25, 30, 60, 90, 120, 150 and 180 minutes), aliquots were collected, filtered and analyzed in a Varian 200 series (AA240p) atomic absorption spectrometer at 223.46 nm, in order to determine the adsorption equilibria time. The same analytical method was used for both samples.

Removal efficiency for Cu²⁺ was calculated by Equation 1.

$$R = \left(\frac{C_i - C_e}{C_i} \right) \times 100 \quad (1)$$

where: R = removal efficiency (%); C_i = initial concentration (mg L⁻¹); C_e = equilibrium concentration (mg L⁻¹);

Adsorption capacity was determined by Equation 2.

$$q = \frac{(C_o - C_e)V}{m} \quad (2)$$

where: q = adsorption capacity (mg g⁻¹); V = solution volume (L); m = biosorbent mass (g)

In order to determine the ideal mass of adsorbent for the adsorption tests, 6 replicates of 50 mL from a 50 g L⁻¹

solution of Cu²⁺ were analyzed. The added mass of biochar to the solutions varied from 0.1 to 0.6 g. The mixtures were kept under continuous stirring for 30 min at 150 rpm. After that period, the solutions were filtered and the remaining content of Cu²⁺ in the aqueous phase was determined by atomic absorption spectrophotometry. In turn, the ideal pH for adsorption was determined as follows. Five portions of 50 mL from a 50 g L⁻¹ solution of Cu²⁺ were taken and pH was adjusted from 2.0 to 6.0. Biochar samples weighing 0.4 g were added to each portion of solution and stirred magnetically for 30 min at 150 rpm. After this, the remaining content of Cu²⁺ in the liquid phase was measured by atomic absorption spectrophotometry.

Adsorption isotherms

Adsorption isotherms were adjusted at three different temperatures (298, 308 and 318 °K) with the concentration of Cu²⁺ varying from 50 to 250 ppm. For this, a solution of 0.4 g of biosorbent in 50 mL of Cu²⁺ was used under continuous stirring at 150 rpm until sorbent-sorbate equilibrium was reached. Both linear Langmuir and Freundlich isotherms were fitted to the experimental data by using the software Excel.

Adsorption isotherms for mixture of metals

Adsorption isotherms were obtained at room temperature (298 °K) by using 50 mL of solution containing Cu²⁺ (copper sulfate pentahydrate), Ni²⁺ (nickel sulfate hexahydrate) and Cd²⁺ (cadmium sulfate hydrate) with concentrations varying in the range of 50 to 250 ppm for each cation. From this point on, these metallic cations will be called s Cu, Ni and Cd to correspond to their cationic form, without the positive charges associated with the element name. All the reagents were high-purity quality purchased from Merck (Darmstadt, Germany). To evaluate the adsorption capacity, 0.5 and 0.4 g of fresh and H₂O₂-treated biochar were used, respectively. Linear Langmuir and Freundlich isotherms were fitted to the experimental data by using the Excel.

Thermodynamic parameters

Thermodynamic parameters were ascertained by carrying out several assays with different concentrations of Cu, varying from 50 to 250 ppm at 25, 35 and 45 °C and using 0.4 g of biosorbent in 50 mL of solution. The solutions were maintained under constant stirring during 30 min at 150 rpm. Variation of Gibbs free energy of mixing, enthalpy and entropy were determined.

Results and Discussion

Fresh and H₂O₂-treated biochar characterization Thermogravimetric analysis

Figure 1 shows the TGA and DTG curves obtained for fresh and H₂O₂-treated biochar. It is possible to identify the beginning of thermal degradation with the corresponding peaks related to moisture loss. The moisture loss peak of the H₂O₂-treated biochar was lower than of the fresh biochar,

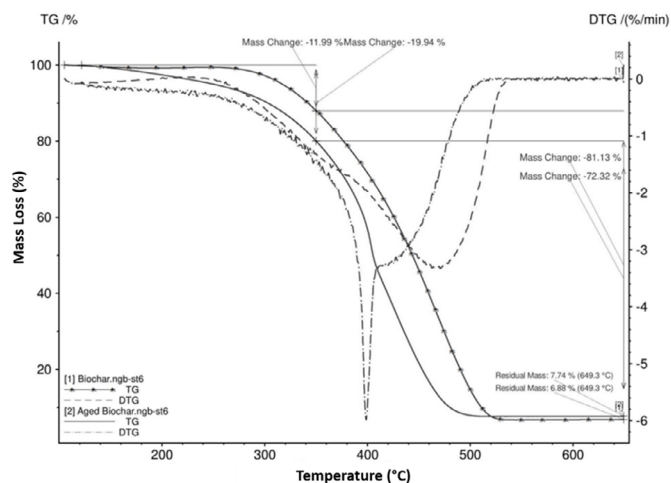


Figure 1. Thermogravimetric (TGA) and derivative (DTG) curves obtained for fresh and H₂O₂-treated biochar.

results similar to those reported by Kucerík et al. (2004) and Cazetta et al. (2011). The second peak is related to the degradation of volatile parts present in higher concentrations in the molecules of the H₂O₂-treated biochar, indicating that during the oxidation reaction, groups with low thermal resistance such as carboxyl, hydroxyl and carbonyl were added to the material, as reported by Trompowsky et al. (2005) and Cazetta et al. (2011). In the DTG curve obtained for fresh biochar, the mass loss is gradual, reaching its maximum at about 480 °C. On the other hand, for H₂O₂-treated biochar, a strong mass loss is observed at 400 °C, indicating volatilization of functional groups at that temperature.

Thermogravimetric indexes (TGI) for both fresh and H₂O₂-treated biochar samples are shown in Table 1. As can be seen for H₂O₂-treated biochar, the area under the curve in the range of 105-350 °C increased in comparison to the fresh biochar, implying that during the oxidation reaction, some alkyl groups were incorporated into the pristine structure. As pointed out by Benites et al. (2005), thermogravimetric index is a direct reflection of the proportion between aryl and alkyl structures. Therefore, a higher TGI reflects a greater amount of aryl structures in the material, and consequently a lower the amount of alkyl ones. According Turčániová et al. (2000), natural and artificial oxidation of biochar usually results in the introduction of oxygenated functional groups in the

Table 1. Thermogravimetric indexes obtained for fresh and H₂O₂-treated biochar.

Biosorbent	Temperature range (°C)		TGI
	105 – 350	350 – 650	
Fresh biochar	12.07	81.46	6.75
H ₂ O ₂ -treated biochar	19.61	71.38	3.64

Table 2. Elemental analysis of fresh and H₂O₂-treated biochar.

Biosorbent	Elemental Composition (%)				
	Carbon	Hydrogen	Oxygen	Nitrogen	Sulfur
Fresh biochar	72.78 a	3.63 a	23.23 a	0.32 a	0.043 a
H ₂ O ₂ -treated biochar	61.00 b	3.52 b	35.19 b	0.25 b	0.042 a

Means followed by different letters in columns are statistically different by the F-test at 95% significance.

chemical structure of the material, such as carboxyl, hydroxyl and carbonyl groups. The TGI parameter can give numbers to the extent of chemical oxidation of biochar, as reported by Trompowsky et al. (2005). In the present experiment, TGI for H₂O₂-treated biochar was 46.0% lower than for the fresh biochar, which most likely indicated a significant increase in the content of functional groups in its structure.

Elemental analysis

Elemental analysis, shown in Table 2, revealed the significant inclusion of oxygen in the composition of biochar during oxidation, which likely can be attributed to an increase of functional groups in the chemical structure. As result of the action of hydrogen peroxide, the oxygen content increased by about 51.5% compared to the fresh biochar's elemental composition. The variation in the contents of hydrogen and nitrogen were small, while there was no statistical change in the content of sulfur when biochar samples before and after oxidation were compared by the F-test.

BET specific surface area and point of zero charge (PZC)

Table 3 reports the results of BET specific surface area obtained for fresh and H₂O₂-treated biochar. The oxidizing reaction with hydrogen peroxide caused a decrease in the surface area of the biochar, confirming the results of the morphological analysis in which no visible changes in the porous structure were detected in the H₂O₂-treated compared to the fresh biochar. However, the results of elemental analysis reveal that a clear change in chemical composition occurred, although no apparent physical alterations occurred due to the oxidation reaction. Figure 2 shows the scanning electron microscopy images for both biochar (A) and H₂O₂-treated biochar (B). It can be seen that the oxidation of biochar caused an increase in pore diameter, which caused a decrease in pore number and resulted in a decrease in surface area, as shown in the BET analysis. The destruction of the cell wall during the oxidation process may be related to the decrease in biochar carbon content, while the increase in oxygen content may be explained by the formation of functional groups on the material surface, as already reported by others researchers (Yao et al., 2016; Güzel et al., 2017; Jin et al., 2018).

Table 3. BET specific surface area of fresh and H₂O₂-treated biochar.

Biosorbent	BET surface area (m ² g ⁻¹)
Fresh biochar	13.8
H ₂ O ₂ -treated biochar	3.6

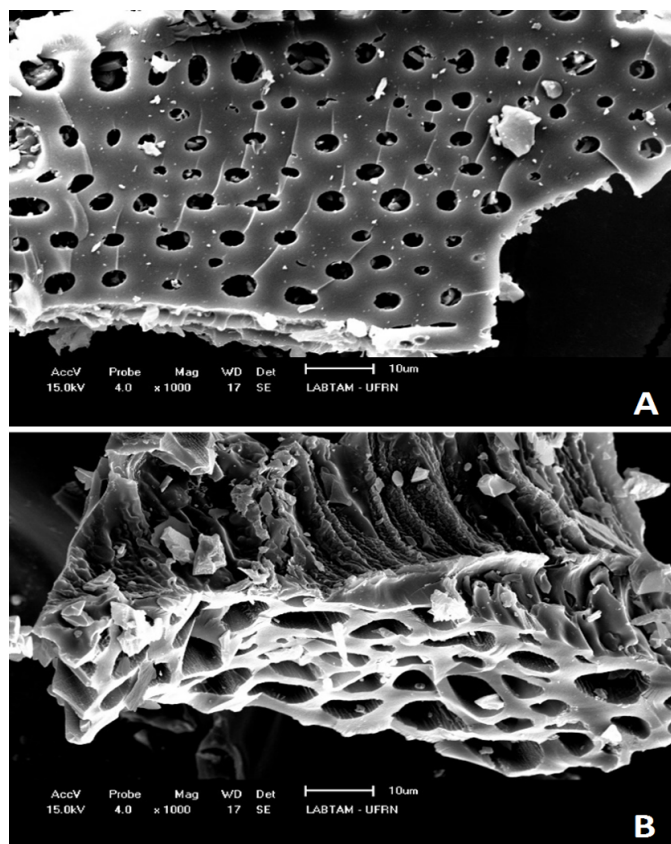


Figure 2. Scanning electron microscopy of fresh biochar (A) and H₂O₂-treated biochar (B).

Other authors have reported a decrease in the surface area after oxidation of biochar (Guo et al., 2014; Frišták et al., 2015). Those researcher groups also found a decrease in the adsorption of Cu by biochar after oxidation, attributing the effect to the addition of functional groups and the decrease in the surface area. In this work, the biochar aging process contributed to the significant increase in its adsorption capacity, these results are in agreement with the results obtained by other researchers, who state that during the carbon oxidation process, functional groups (carboxylates, phenols and CO bonds) are inserted on the surface of the material, which implies increasing its adsorption capacity, due to increased electrostatic attraction, caused by increased total surface acidity of the material (Güzel et al., 2017; Spessato et al., 2019; Eeshwarasinghe et al., 2019).

Figure 3 shows the point of zero charge obtained for fresh and H₂O₂-treated biochar. Usually, the biosorbent surface is positively charged in the range where solution pH is lower than the PZC, due to the protonation in acid media. As pH increases, the functional groups are progressively deprotonated, which allows reaction with metallic cations, as discussed by Silva et al. (2018). As pointed out by those authors, solution pH is one of the most important factors affecting the adsorption phenomenon, since it directly affects the solubility of metallic salts. When a biosorbent is deprotonated, the electrostatic affinity between positive charges of metallic cations and the negative charge sites in the substrate is maximized, resulting

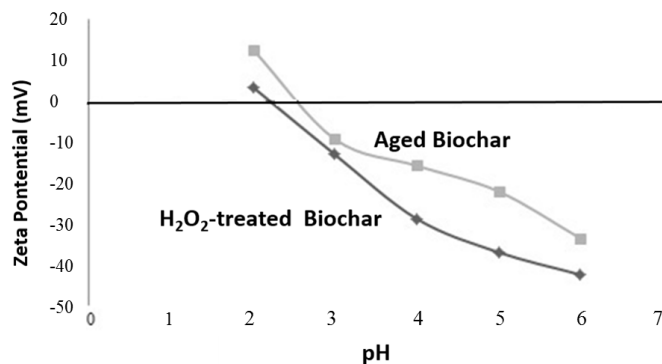


Figure 3. Point of zero charge for fresh and H₂O₂-treated biochar.

in higher removal of metals from aqueous solutions. The PZC is the point where the biosorbent reaches its minimum net charge, which is important to define the best conditions to use the product. In other words, the PZC shows the ability of a given substrate to adsorb cations or anions, as a function of pH at a given temperature (Nascimento et al., 2014; González-García, 2018). The PZC values were 2.15 and 2.50 for fresh and H₂O₂-treated biochar, respectively.

Although there are already some studies showing the effects of biochar modification with H₂O₂, studies of modification mechanisms that reflect the improvement in adsorption capacity are still scarce, as stated by Zuo et al. (2016). According to Guo et al. (2014), phenolic hydroxyl groups increase after the biochar oxidation process, which makes it more difficult to dissociate these groups at pH ranging from 5 to 6.8, as in this work, the same happens with carboxyl groups. The modification mechanism occurs in the chemical composition of the surface of the material, with the significant increase and modification in functional groups, which increases the adsorption capacity of biochar, since the change in surface structure pointed by the SEM was not so noticeable and the specific area of the material decreased (Guo et al., 2014; Zuo et al., 2016; Wang & Liu, 2018).

According to Swiatkowski et al. (2004), the main mechanism of biochar metal adsorption is the complexation, which occurs between heavy metals and ionized oxygenated functional groups. Wang & Liu (2018) also discuss the complexation mechanism proposed by Swiatkowski et al. (2004) justifying the increase in adsorption capacity due to the occurrence of this mechanism after modification with H₂O₂ which resulted in significant increase of carboxyl groups. As shown by Li et al. (2014), besides the image analysis used in this work, infrared spectroscopy is a method that can help in understanding the modification and adsorption mechanisms of charcoal, with this analysis it is possible to build grounded explanations about the chemical processes that occur in biochar, as the authors did with aluminum-impregnated bone charcoal.

Adsorption kinetics tests with Cu

In the test of adsorption of Cu by fresh biochar, the equilibrium was reached only after 30 min and the removal of this metallic cation from the aqueous solution barely

exceeded 50%. On the other hand, in the adsorption test carried out with H₂O₂-treated biochar, an equilibrium time of only 1 min was observed, as shown in Figure 4, indicating a higher affinity between the biosorbent and metallic cations comparing to the fresh biochar. Even when left to interact for a longer time to reach equilibrium, fresh biochar had lower adsorption. In the present work, even though the sorbent-sorbate equilibrium was reached in only 1 min, the contact time was kept at 30 min. However, even so there were no changes in the adsorption before equilibrium was reached, with a respective Cu removal higher than 99% by the H₂O₂-treated biochar.

Since H₂O₂-treated biochar was more efficient than fresh biochar in the removal of Cu, the effect of mass variation on the potential adsorption was assessed. The results are shown in the Figure 5. As can be seen, the variation of mass of the biosorbent in the range from 0.2 to 0.6 g showed that an amount of 0.4 g had the same potential to adsorb 0.5 or 0.6 g. This result is technically and economically important, since a limit for utilization of the biosorbent per volume of aqueous solution can be established as a function of its removal efficiency. In the present experiment, the removal exceeded 99%.

Among the factors affecting adsorption capacity of H₂O₂-treated biochar, pH was the main influence on that parameter, as can be seen in Figure 6. At pH 2, the removal of Cu was of

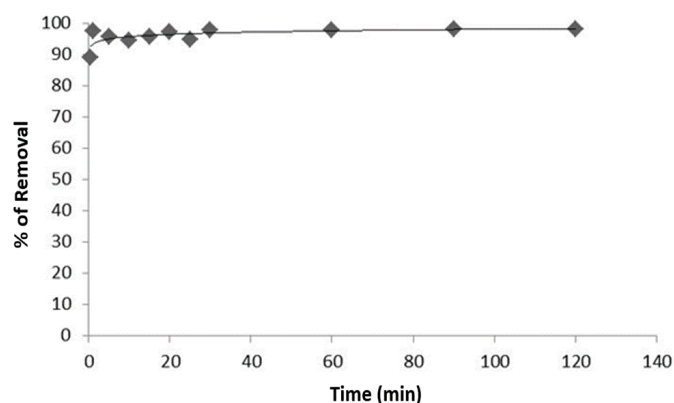


Figure 4. Equilibrium time for Cu adsorption by H₂O₂-treated biochar.

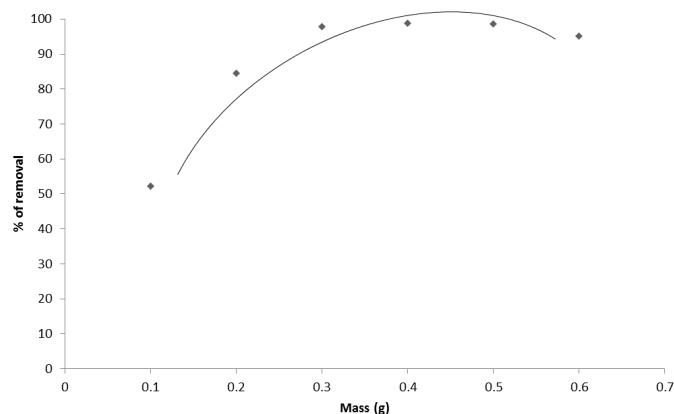


Figure 5. Effect of the mass variation of H₂O₂-treated biochar on the potential adsorption of Cu.

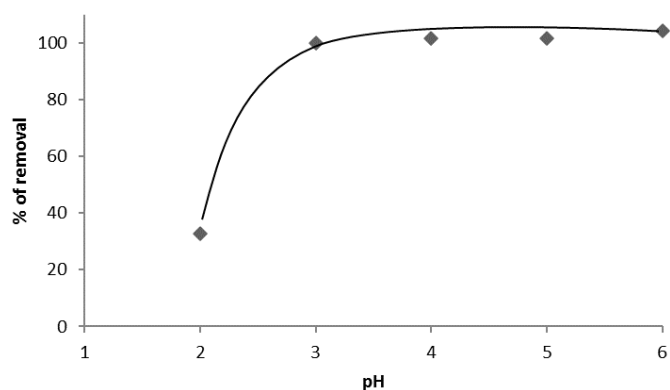


Figure 6. Effect of pH on the adsorption capacity of H₂O₂-treated biochar.

only 32%, while the adsorption capacity did not vary at pH equal to 4, 5 and 6, almost reaching 100% efficiency in that range. The low adsorption at pH 2.0 is a coherent result, since that value coincides very closely with the PZC value cited above. As discussed, close to the PZC, most functional groups are protonated, which makes it harder for the biosorbent to interact with metallic cations.

As cited in the literature, only a few adsorbents have satisfactory adsorption capacity in aqueous solutions with pH higher than 7, regardless of the precursor and the adsorption activating agent (Luna et al., 2013; Angin, 2014; Ghaedi et al., 2015). According to those authors, the predominant adsorption capacity occurs mostly in acid media. In the present experiment, the adsorption efficiency of H₂O₂-treated biochar indicated that the oxidation with hydrogen peroxide was able to add functional groups to the structure of biochar, and those groups were responsible for the faster removal of Cu, as observed in the adsorption tests, compared to the fresh biochar at the same pH and temperature. Results of adsorption tests reported by Domingues (2005) and Nascimento et al. (2014) with similar materials corroborate that added oxygenated functional groups are determinant in the adsorption behavior.

Adsorption isotherms for Cu

The graph in Figure 7A is plotted from the data for the Langmuir isotherms, showing the concentration (C_e) of Cu in equilibrium in the solution as a function of the ratio between the amount of adsorbed copper in the biosorbent and the cation concentration in solution (C_e/q_e). In Figure 7B, the graph was constructed with data from the Freundlich isotherms, showing ratio between log q_e and log C_e.

The maximum adsorption capacity values (q_m) predicted by using the Langmuir isotherm are shown in Table 4. The table also reports experimental maximum adsorption capacity found in the present work (q_{exp}), the Langmuir constant (b), the dimensionless separation factor (k_L) and the correlation coefficient (R²). Finally, the table shows the values obtained for the Freundlich constants (K_F and n) and the correlation coefficient (R²) of the fit.

The Langmuir model presupposes that sorbate adsorption occurs with the formation of monolayers and that the sorbent

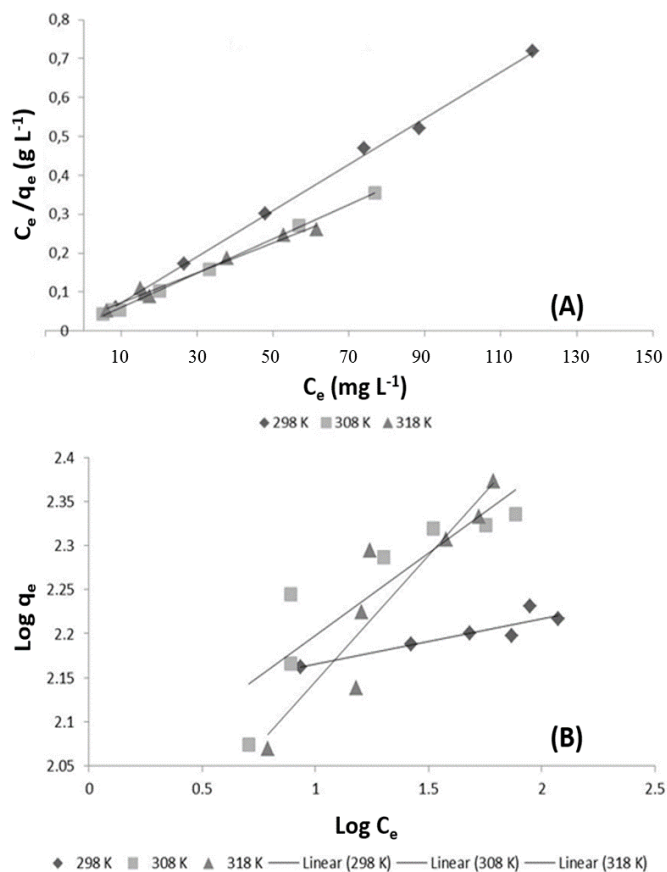


Figure 7. Langmuir (A) and Freundlich (B) isotherms for Cu adsorption with H₂O₂-treated biochar.

surface is homogeneous (Gode & Pehlivan, 2005). At the temperature of 298 °K, the isotherm that best fit the Cu adsorption by the H₂O₂-treated biochar was the Langmuir, with a correlation coefficient of 0.9976, compared to 0.8275 for the Freundlich isotherm. The dimensionless separation factor (KL), which is related to the free energy of adsorption and reflects the affinity between the sorbent surface and the sorbate, can indicate whether the isotherm is appropriate for prediction (Nascimento et al., 2014). According to those authors, the KL value must be in the range of 0 and 1 (0 < KL < 1), which occurred in the present experiment, where the lowest value was 0.013 and the highest was 0.054.

The value to the maximum adsorption capacity predicted by the Langmuir isotherm (169.49 mg g⁻¹) was very close

to the experimental value (170.41 mg L⁻¹), indicating good adjustment of the model to the adsorption behavior of the H₂O₂-treated biochar. This was further supported by the value of the correlation coefficient. In general, the better the adsorbent, the higher the values of q_m and K_L will be, as described by Nascimento et al. (2014). With respect to the Freundlich isotherm data showed in Table 4, when the value of 1/n is in the range of 0 and 1 (as occurred in the present work, where the lowest value was 0.05 and the highest was 0.29), the adjusted model is considered appropriate to explain the adsorption phenomenon (Nascimento et al., 2014). While n is related to the adsorption intensity between the sorbate and the adsorbent, K_F is related to the adsorption capacity of the adsorbent. In this experiment, the highest value found for K_F was 2.1143 and the lowest was 1.8602, both of which are higher than the values reported by Melo (2012) for the adsorption of Cu, respectively, 1.03 in a linear model and 1.47 in a nonlinear one.

Adsorption isotherms for a mixture of metallic cations

When the fresh biochar was evaluated in a solution containing more than one metallic cation, the results showed different patterns for the adsorption preference. Figures 8A and 8B, respectively, show the Langmuir and Freundlich isotherms. This time, the isotherms were adjusted to explain the behavior of biochar in the adsorption of metallic cations from a solution containing Cu, Cd and Ni. Except for Cu, the model that showed the best fit was Langmuir, with correlation coefficients of 0.9939 and 0.9750 for Cd and Ni, respectively. According to Nascimento et al. (2014), when the mass of adsorbate retained per unit of mass of adsorbent is high for a low concentration of adsorbate in equilibrium, the isotherm is said to be favorable. On the other hand, when the mass of adsorbate retained per unit mass of the adsorbent is low, even for a high equilibrium concentration of the adsorbate, the isotherm is classified as unfavorable.

Isotherm parameters are shown in Table 5. When compared to the adsorption parameters obtained for H₂O₂-treated biochar (Table 6), the adsorption capacity values of the fresh biochar are much lower. This result was expected, since a similar trend was observed in the adsorption of Cu as a single cation. It is also possible to observe that the best adsorption of the fresh biochar occurred for Cd, followed by

Table 4. Parameters of the adjusted isotherms for the adsorption of Cu by H₂O₂-treated biochar.

Isotherm	Parameter					
	Temperature (°K)	q _m (mg g ⁻¹)	B (L mg ⁻¹)	K _L	q _{exp} (mg L ⁻¹)	R ²
Langmuir	298	169.49	0.44	0.013	170.41	0.9976
	308	216.44	0.28	0.022	227.27	0.9993
	318	235.77	0.11	0.054	263.16	0.9824
Freundlich	Temperature (°K)	K _F	1/n	R ²		
	298	2.1143	0.05	0.8275		
	308	2.011	0.19	0.7881		
	318	1.8602	0.29	0.8509		

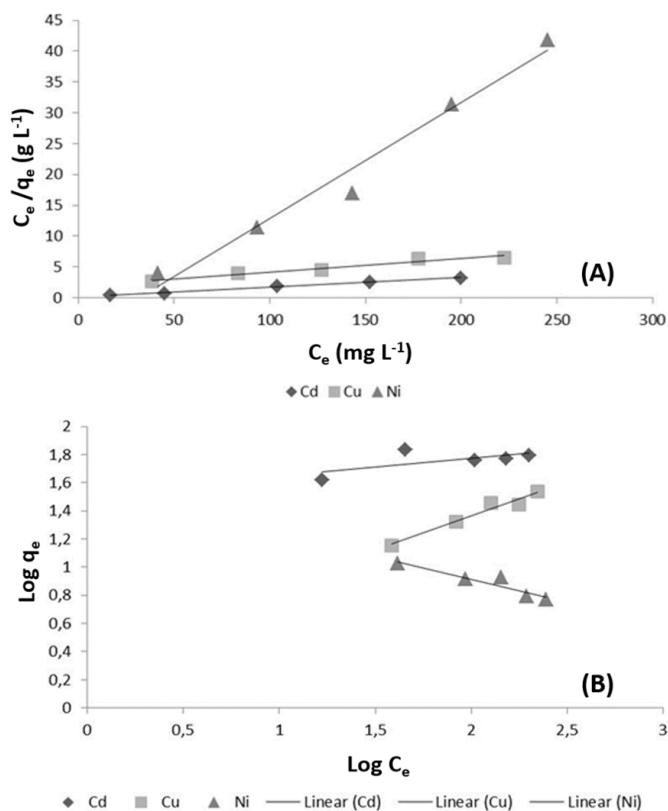


Figure 8. Langmuir (A) and (B) isotherms for the adsorption of Cu, Cd and Ni with fresh biochar.

Cu and Ni. For the H₂O₂-treated biochar, adsorption preference followed the order Cu, Cd and Ni.

The ionic radius of the elements possibly can explain the differences in adsorption order. Cd has a higher ionic radius than Cu and Ni, which could have favored its adsorption by the biochar since in that case the adsorption seems to be mostly a physical

phenomenon. The introduction of oxygenated functional groups on the surface of biochar caused by the oxidation reaction with hydrogen peroxide most likely altered the preferential order of adsorption, since the predominant phenomenon became chemically oriented, behavior also reported by Cheng-Chung et al. (2009) and Nascimento et al. (2014).

Figures 9A and 9B show, respectively, the Langmuir and Freundlich isotherms for the absorption of Cu, Cd and Ni with H₂O₂-treated biochar. Considering the sorbent-sorbate affinity, the highest value of K_L (Table 4) was observed for Cd (0.069). However, the highest adsorption occurred for the ions of Cu, being practically two times higher than that observed for Cd, indicating that despite the stronger interaction with the surface of the H₂O₂-treated biochar, the ionic radius of Cd probably prevented its adsorption in higher amounts, which did not occur in the case of Cu ions. The lowest removal was observed for Ni by both fresh and H₂O₂-treated biochar. In both cases, with a negative values for K_L and $1/n$, the adsorption is indicated as being unfavorable, meaning that the amount of mass retained in the biosorbent does not depend on the equilibrium concentration of the sorbate in the liquid phase, as pointed out by Moreira et al. (2009).

Considering the three cations in the aqueous solution, the best adjustment of the adsorption phenomenon was achieved with the Langmuir isotherm, which showed the best correlation coefficients. As occurred with the fresh biochar, only adsorption of Ni was not classified as having a favorable isotherm, showing negative values for K_L and $1/n$. The maximum adsorption capacity when added to the individual adsorption of each metal reached 113.39 and 305.35 mg g⁻¹ for fresh and H₂O₂-treated biochar, respectively.

The results found in the present work for the adsorption of Ni by both biosorbents were much lower than those ones

Table 5. Isotherm parameters for the adsorption of a mixture of Cu, Cd and Ni with fresh biochar at 298 °K.

Isotherm	Parameters					
	Cation	q_m (mg g ⁻¹)	B (L mg ⁻¹)	K_L	q_{exp} (mg L ⁻¹)	R^2
Langmuir	Cu	46.08	0.01	0.417	34.31	0.9491
	Ni	5.30	-0.03	-0.549	10.54	0.9750
	Cd	62.89	0.21	0.040	68.54	0.9939
Freundlich	Cation	K_F	$1/n$	R^2		
	Cu	0.399	0.48	0.9617		
	Ni	1.555	-0.32	0.8786		
	Cd	1.528	0.12	0.4293		

Table 6. Isotherm parameters for the adsorption of a mixture of Cu, Cd and Ni with H₂O₂-treated biochar at 298 °K.

Isotherm	Parameter					
	Cation	q_m (mg g ⁻¹)	B (L mg ⁻¹)	K_L	q_{exp} (mg L ⁻¹)	R^2
Langmuir	Cu	178.57	0.17	0.050	176.25	0.9924
	Ni	9.01	-0.03	-0.535	41.15	0.9728
	Cd	83.33	0.12	0.069	87.95	0.9996
Freundlich	Cation	K_F	$1/n$	R^2		
	Cu	1.530	0.83	0.7830		
	Ni	2.331	-0.56	0.9637		
	Cd	1.486	0.20	0.3751		

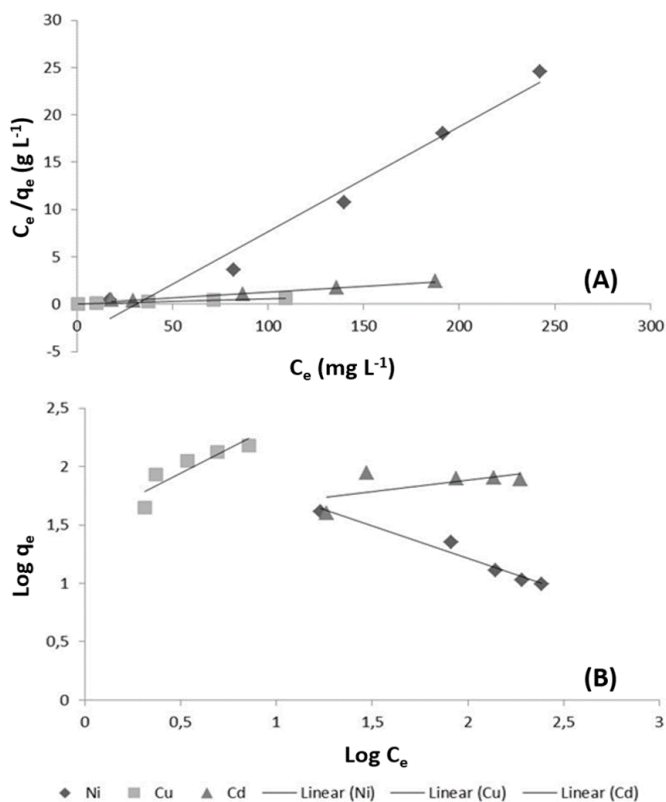


Figure 9. Langmuir (A) and Freundlich (B) isotherms for the adsorption of Cu, Cd and Ni with H₂O₂-treated biochar.

achieved with activated charcoal by Rodriguez et al. (2018). They employed coffee husks as raw material and a classic activation process at high temperatures. They obtained maximum adsorption of 51.94 mg g⁻¹. Regarding Cd, in the present experiment higher adsorption was achieved compared to the results of Feng et al. (2018), who reported maximum adsorption capacity in the range from 36.95 to 49.11 mg g⁻¹. Those authors evaluated charcoal from wastes of Astragalus activated with potassium permanganate. As observed here, when more than one cation was present in the aqueous solution, the adsorption capacity of the biosorbents increased in comparison to the situations with single cations in solution.

Thermodynamic adsorption parameters

Figure 10 shows a graph plotted with values of temperature vs. equilibrium constant for H₂O₂-treated biochar. As in Table 7, thermodynamic parameters (respectively enthalpy, entropy and Gibbs free energy) are presented.

When in linearized form, the values for the equilibrium constant (Ln Kd) and temperature (1/T), respectively, permit calculating the variation in the thermodynamic parameters by means of the equation of a line. Those parameters are important to understand how spontaneous the adsorption phenomenon is, and also to provide information about its behavior, according Nascimento et al. (2014). In that sense, Robati et al. (2016) emphasized that if the value of enthalpy variation is positive, an endothermic adsorption process occurred, unlike the result of the present work. In turn, a negative value for Gibbs free energy indicates that

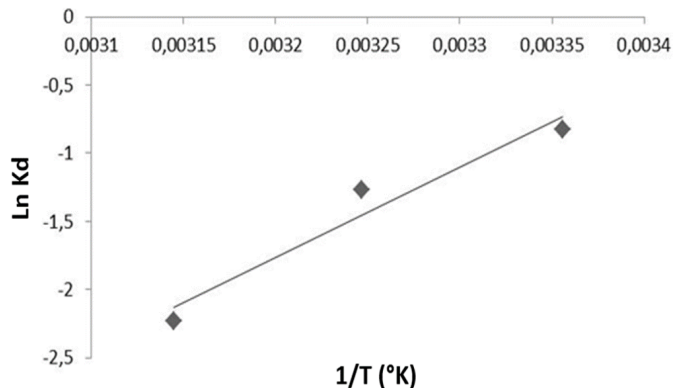


Figure 10. Adsorption temperature vs. equilibrium constant for H₂O₂-treated biochar.

Table 7. Thermodynamic parameters for Cu adsorption by H₂O₂-treated biochar.

Temperature (°K)	ΔH° (KJ mol ⁻¹)	ΔS° (KJ mol ⁻¹ °K ⁻¹)	ΔG° (KJ mol ⁻¹)
298	-54.95	0.191	-111.86
308	-54.95	0.191	-113.78
318	-54.95	0.191	-115.69

ΔH° = Enthalpy variation; ΔS° = Entropy variation; ΔG° = Gibbs free energy variation

the adsorption is spontaneous, which was observed in the present work and was reported by Dirbaz & Roosta (2018) and Pandiarajan et al. (2018). Positive values for entropy, as shown here, indicate an increase of the system's disorder during the adsorption process at the sorbent-solution interface (Karthikeyan et al., 2012; Pandiarajan et al., 2018).

Comparison of H₂O₂-treated biochar with activated charcoal

Table 8 presents comparison of H₂O₂-treated biochar obtained in the present work and the results reported by some other authors for specific surface area and heavy metals adsorption capacity of activated charcoals obtained from several lignocellulosic raw materials. As can be observed, H₂O₂-treated biochar from eucalyptus had the lowest surface area but the highest adsorption capacity. Naturally, the comparison is mostly illustrative since the experimental conditions and the metallic cations are not exactly the same as in our study, but even so, the data in Table 8 show the good potential of H₂O₂-treated biochar from eucalyptus as an efficient biosorbent. Other advantages of the H₂O₂-treated biochar are the use of hydrogen peroxide for chemical oxidizing (only generating oxygen as gaseous byproduct) and the mild reaction conditions regarding pH and temperature. These aspects make the oxidizing procedure easy since no complex equipment is needed and none toxic effluents are released by the process. Furthermore, the values for adsorption of Cu and Cd found in the present work for H₂O₂-treated biochar are higher than the results found by Chaudhuri et al. (2010). They reported adsorptions of 84.74 and 68.03 mg g⁻¹, respectively, for Cu and Cd, by activated charcoal prepared from coconut coir and adsorptions of 46.30 and 14.90 mg g⁻¹ for a commercial activated charcoal.

Table 8. Comparison of surface area and adsorption capacities for activated charcoals and H₂O₂-treated biochar.

Precursor	Activation agent	Surface area (m ² g ⁻¹)	Adsorption capacity (mg g ⁻¹)	Reference
<i>B. vulgaris striata</i>	Steam	608	239.45	González & Pliego-Cuervo (2014)
Coconut shell	HNO ₃	647	20.2	Gu et al. (2019)
<i>Glycyrrhiza glabra</i>	ZnCl ₂	1483	200	Mohammadi et al. (2014)
Grape bagasse	H ₃ PO ₄	1455	43.47	Demiral & Güngör (2016)
Hickory	NaOH	873	53.6	Ding et al. (2016)
Longan seed	NaOH	1512	169.5	Yang et al. (2015)
<i>Posidonia oceanica</i>	H ₃ PO ₄	946.55	137.3	Ncibi et al. (2014)
<i>Posidonia oceanica</i>	H ₂ O ₂	60.24	49.04	Ncibi et al. (2014)
Eucalyptus aged biochar	H ₂ O ₂	3.6	270.91	Present work

Taking into consideration all results presented and discussed here, the technical viability of the use of H₂O₂-treated biochar for removal of Cu and Cd seems to be feasible, since for Ni the removal was equally efficient as for the other cations. In Brazil, large amounts of eucalyptus charcoal are produced throughout the year. From the standpoint of adding value to the forest industry by transforming part of the yearly supply of charcoal into biochar, a large source of renewable raw material would be ready to use.

Conclusions

Treatment of biochar with H₂O₂ is a favorable process from both technical and environmental perspectives.

A relatively low concentration of reagent combined with mild reaction conditions were required, providing a high-efficiency product with performance comparable to biosorbents cited in the literature for the removal of heavy metals from aqueous solution.

The H₂O₂ treatment process caused a significant decrease of surface area in the biochar, but even so the H₂O₂-treated product showed superior adsorption capacity in relation to the original raw material.

Despite having a much lower surface area compared to usual activated charcoals, H₂O₂-treated biochar was effective for the adsorption of Cu and Cd, since the process was able to add oxygenated functional groups in the structure, increasing the adsorption capacity.

When tested in the presence of more than one metal, H₂O₂-treated biochar's adsorption capacity improved significantly, indicating the possibility of applying it as a biosorbent in complex mixtures.

Acknowledgements

This study was financed in part by the Coordenação de Aperfeiçoamento de Pessoal de Nível Superior - Brasil (CAPES) - Finance Code 001. This work was supported by the Graduate Program in Forest Science (PPGCFL) of Rio Grande do Norte Federal University (UFRN, Brazil), NUPEG and the Nucleus for Primary Processing and Reuse of Produced Water and Waste (NUPPRAR). We are especially grateful to Ibiré Sustainable Business Ltd. for financial support and supplying analytical material and chemical reagents.

Literature Cited

- Aller, D.; Rathke, S.; Laird, D.; Cruse, R.; Hatfield, J. Impacts of fresh and aged biochars on plant available water and water use efficiency. *Geoderma*, v.307, p.114-121, 2017. <https://doi.org/10.1016/j.geoderma.2017.08.007>.
- Angin, D. Utilization of activated carbon produced from fruit juice industry solidwaste for the adsorption of Yellow 18 from aqueous solutions. *Bioresource Technology*, v.168, p.259-266, 2014. <https://doi.org/10.1016/j.biortech.2014.02.100>.
- Benites, V.M.; Mendonça, E.S.; Schaefer, C.E.G.R.; Novotny, E.H.; Reis, E.L.; Ker, J.C. Properties of black soil humic acids from high altitude rock complexes in Brazil. *Geoderma*, v.127, n.1-2, p.104-113, 2005. <https://doi.org/10.1016/j.geoderma.2004.11.020>.
- Brazilian Tree Industry – BTI. Report 2017. São Paulo: IBÁ, 2017. 77p. <https://www.iba.org/datafiles/publicacoes/pdf/iba-relatorioanual2017.pdf>. 07 Mar. 2019.
- Cazetta, A.L.; Vargas, A.M.M.; Nogami, E.M.; Kunita, M.H.; Guilherme, M.R.; Martins, A.C.; Silva, T.L.; Moraes, J.C.G.; Almeida, V.C. NaOH-activated carbon of high surface area produced from coconut shell: kinetics and equilibrium studies from the methylene blue adsorption. *Chemical Engineering Journal*, v.174, n.1, p.117-125, 2011. <https://doi.org/10.1016/j.cej.2011.08.058>.
- Chaudhuri, M.; Kutty, S.R.M.; Yusop, S.H. Copper and cadmium adsorption by activated charcoal from coconut coir. *Nature Environment and Pollution Technology*, v.9, n.1, p.25-28, 2010. [http://neptjournal.com/upload-images/NL-3-4-\(4\)B-1456.pdf](http://neptjournal.com/upload-images/NL-3-4-(4)B-1456.pdf). 10 Mar. 2019.
- Cheng, C.H.; Lehmann, J. Aging of black carbon along a temperature gradient. *Chemosphere*, v.75, n.8, p.1021-1027, 2009. <https://doi.org/10.1016/j.chemosphere.2009.01.045>.
- Cheng, C.-H.; Lehmann, J.; Engelhard, M.H. Natural oxidation of black carbon in soils: changes in molecular form and surface charge along a climosequence. *Geochimica et Cosmochimica Acta*, v.72, n.6, p.1598-1610, 2008. <https://doi.org/10.1016/j.gca.2008.01.010>.
- Cheng-Chung, L.; Ming-Kuang, W.; Chyow-San, C.; Yuan-Shen, L.; Chia-Yi, Y.; Yu-An, L. Biosorption of chromium, copper and zinc by wine-processing waste sludge: Single and multi-component system study. *Journal of Hazardous Materials*, v.171, n.1-3, p.386-392, 2009. <https://doi.org/10.1016/j.jhazmat.2009.06.012>.
- Demiral, H.; Güngör, C. Adsorption of copper (II) from aqueous solutions on activated carbon prepared from grape bagasse. *Journal of Cleaner Production*, v.124, p.103-113, 2016. <https://doi.org/10.1016/j.jclepro.2016.02.084>.

- Ding, Z.; Hu, X.; Wan, Y.; Wang, S.; Gao, B. Removal of lead, copper, cadmium, zinc, and nickel from aqueous solutions by alkali-modified biochar: Batch and column tests. *Journal of Industrial and Engineering Chemistry*, v.33, p.239-245, 2016. <https://doi.org/10.1016/j.jiec.2015.10.007>.
- Dirbaz, M.; Roosta A. Adsorption, kinetic and thermodynamic studies for the biosorption of cadmium onto microalgae *Parachlorella* sp. *Journal of Environmental Chemical Engineering*, v.6, n.2, p.2302-2309, 2018. <https://doi.org/10.1016/j.jece.2018.03.039>.
- Domingues, V.M.F. Utilização de um produto natural (cortiça) como adsorvente de pesticidas piretróides em águas. Porto: Universidade do Porto, 2005. 198p. PhD Thesis. <https://hdl.handle.net/10216/12811>. 28 Feb. 2019.
- Eshwarasinghe, D.; Loganathan, P.; Vigneswaran, S. Simultaneous removal of polycyclic aromatic hydrocarbons and heavy metals from water using granular activated carbon. *Chemosphere*, v. 223, p.616-627, 2019. <https://doi.org/10.1016/j.chemosphere.2019.02.033>.
- Feng, N.; Fan, W.; Zhu, M.; Guo, X. Adsorption of Cd²⁺ in aqueous solutions using KMnO₄-modified activated carbon derived from *Astragalus* residue. *Transactions of Nonferrous Metals Society of China*, v.28, n.4, p.794-801, 2018. [https://doi.org/10.1016/S1003-6326\(18\)64712-0](https://doi.org/10.1016/S1003-6326(18)64712-0).
- Frišták, V.; Friesl-Hanl, W.; Wawra, A.; Pipíška, M.; Soja, G. Effect of biochar artificial ageing on Cd and Cu sorption characteristics. *Journal of Geochemical Exploration*, v.159, p.178-184, 2015. <https://doi.org/10.1016/j.gexplo.2015.09.006>.
- Ghaedi, M.; Mazaheri, H.; Khodadoust, S.; Hajati, S.; Purkait, M.K. Application of central composite design for simultaneous removal of methylene blue and Pb²⁺ ions by walnut wood activated carbon. *Spectrochimica Acta Part A: Molecular and Biomolecular Spectroscopy*, v.135, p.479-490, 2015. <https://doi.org/10.1016/j.saa.2014.06.138>.
- Glaser, B.; Lehmann, J.; Zech, W. Ameliorating physical and chemical properties of highly weathered soils in the tropics with charcoal – a review. *Biology and Fertility of Soils*, v.35, p.219-230, 2002. <https://doi.org/10.1007/s00374-002-0466-4>.
- Gode, F.; Pehlivan, E. Adsorption of Cr(III) ions by Turkish brown coals. *Fuel Processing Technology*, v.86, n.8, p.875-884, 2005. <https://doi.org/10.1016/j.fuproc.2004.10.006>.
- González, P.G.; Pliego-Cuervo, Y.B. Adsorption of Cd(II), Hg(II) and Zn(II) from aqueous solution using mesoporous activated carbon produced from *Bambusa vulgaris striata*. *Chemical Engineering Research and Design*, v.92, n.11, p.2715-2524, 2014. <https://doi.org/10.1016/j.cherd.2014.02.013>.
- González-García, P. Activated carbon from lignocellulosics precursors: A review of the synthesis methods, characterization techniques and applications. *Renewable and Sustainable Energy Reviews*, v.82, part 1, p.1393-1414, 2018. <https://doi.org/10.1016/j.rser.2017.04.117>.
- Gu, S.-Y.; Hsieh, C.-T.; Gandomi, Y.A.; Yang, Z.-F.; Li, L.; Fu, C.-C.; Juang, R.-S. Functionalization of activated carbons with magnetic Iron oxide nanoparticles for removal of copper ions from aqueous solution. *Journal of Molecular Liquids*, v.277, p.499-505, 2019. <https://doi.org/10.1016/j.molliq.2018.12.018>.
- Guo, Y.; Tang, W.; Wu, J.; Huang, Z.; Dai, J. Mechanism of Cu(II) adsorption inhibition on biochar by its aging process. *Journal of Environmental Sciences*, v.26, n.10, p.2123-2130, 2014. <https://doi.org/10.1016/j.jes.2014.08.012>.
- Güzel, F.; Saygılı, H.; Saygılı, G.A.; Koyuncu, F.; Yilmaz, C. Optimal oxidation with nitric acid of biochar derived from pyrolysis of weeds and its application in removal of hazardous dye methylene blue from aqueous solution. *Journal of Cleaner Production*, v.144, p.260-265, 2017. <https://doi.org/10.1016/j.jclepro.2017.01.029>.
- Jin, J.; Li, S.; Peng, X.; Liu, W.; Zhang, C.; Yang, Y.; Han, L.; Du, Z.; Sun, K.; Wang, X. HNO₃ modified biochars for uranium (VI) removal from aqueous solution. *Bioresource Technology*, v.256, p.247-253, 2018. <https://doi.org/10.1016/j.biortech.2018.02.022>.
- Karthikeyan, S.; Gupta, V.K.; Boopathy, R.; Titus, A.; Sekaran, G. A new approach for the degradation of high concentration of aromatic amine by heterocatalytic Fenton oxidation: kinetic and spectroscopic studies. *Journal of Molecular Liquids*, v.173, p.153-163, 2012. <https://doi.org/10.1016/j.molliq.2012.06.022>.
- Köseoğlu, E.; Akmil-Başar, C. Preparation, structural evaluation and adsorptive properties of activated carbon from agricultural waste biomass. *Advanced Powder Technology*, v.26, n.3, p.811-818, 2015. <https://doi.org/10.1016/j.apt.2015.02.006>.
- Kucerík, J.; Kovár, J.; Pekar, M. Thermoanalytical investigations of lignite humic acid fractions. *Journal of Thermal Analysis and Calorimetry*, v.76, p.55-65, 2004. <https://doi.org/10.1023/B:JTAN.0000027803.24266.48>.
- Lahori, A.H.; Zhang, Z.; Guo, Z.; Mahar, A.; Li, R.; Awasthi, M.K.; Sial, T.A.; Kumbhar, F.; Wang, P.; Shen, F.; Zhao, J.; Huang, H. Potential use of lime combined with additives on (im) mobilization and phytoavailability of heavy metals from Pb/Zn smelter contaminated soils. *Ecotoxicology and Environmental Safety*, v.145, p.313-323, 2017. <https://doi.org/10.1016/j.ecoenv.2017.07.049>.
- Li, H.; Yang, Y.; Yang, S.; Chen, A.; Yang, D. Infrared spectroscopic study on the modified mechanism of aluminum-impregnated bone charcoal. *Journal of Spectroscopy*, v.2014, article 671956, 2014. <https://doi.org/10.1155/2014/671956>.
- Liu, Z.; Zhang, F.-S. Removal of lead from water using biochars prepared from hydrothermal liquefaction of biomass. *Journal of Hazardous Materials*, v.167, n.1-3, p.933-939, 2009. <https://doi.org/10.1016/j.jhazmat.2009.01.085>.
- Luna, M.D.G.de; Flores, E.D.; Genuino, D.A.D.; Futralan, C.M.; Wan, M.-W. Adsorption of Eriochrome Black T (EBT) dye using activated carbon prepared from waste rice hulls – optimization, isotherm and kinetic studies. *Journal of the Taiwan Institute of Chemical Engineers*, v.44, n.4, p.646-653, 2013. <https://doi.org/10.1016/j.jtice.2013.01.010>.
- Melo, D.Q. Remoção de Cu²⁺ e Zn²⁺ utilizando esferas de sílica funcionalizadas com EDTA: estudo em batelada e coluna. Fortaleza: Universidade Federal do Ceará, 2012. 93p. <http://www.repositorio.ufc.br/handle/riufc/11138>. 10 Mar. 2019.
- Mia, S.; Dijkstra, F.A.; Singh, B. Long-term aging of biochar: a molecular understanding with agricultural and environmental implications. In: Sparks, D.L. (Ed.). *Advances in Agronomy*. Cambridge: Academic Press, 2017. v. 141, Chap. 1, p.1-51. <https://doi.org/10.1016/bs.agron.2016.10.001>.

- Miao, Q.; Tang, Y.; Xu, J.; Liu, X.; Xiao, L.; Chen, Q. Activated carbon prepared from soybean straw for phenol adsorption. *Journal of the Taiwan Institute of Chemical Engineers*, v.44, n.3, p.458–465, 2013. <https://doi.org/10.1016/j.jtice.2012.12.006>.
- Mohammadi, S.Z.; Hamidian, H.; Moeinadini, Z. High surface area-activated carbon from *Glycyrrhiza glabra* residue by ZnCl₂ activation for removal of Pb(II) and Ni(II) from water samples. *Journal of Industrial and Engineering Chemistry*, v.20, n.6, p.4112–4118, 2014. <https://doi.org/10.1016/j.jiec.2014.01.009>.
- Moreira, S.A.; Sousa, F.W.; Oliveira, A.G.; Nascimento, R.F. do; Brito, E.S. Remoção de metais de solução aquosa usando bagaço de caju. *Química Nova*, v. 32, n.7, p.1717–1722, 2009. <https://doi.org/10.1590/S0100-40422009000700007>.
- Nascimento, R.F. do; Lima, A.C.A. de; Vidal, C.B.; Melo, D. de Q.; Raulino, G.S.C. Adsorção: aspectos teóricos e aplicações ambientais. *Fortaleza: Imprensa Universitária*, 2014. 256p. <http://www.repositorio.ufc.br/handle/riufc/10267>. 08 Mar. 2019.
- Ncibi, M.C.; Ranguin, R.; Pintor, M.J.; Jeanne-Rose, V.; Sillanpää, M.; Gaspard, M. Preparation and characterization of chemically activated carbons derived from Mediterranean *Posidonia oceanica* (L.) fibres. *Journal of Analytical and Applied Pyrolysis*, v.109, p.205–214, 2014. <https://doi.org/10.1016/j.jaap.2014.06.010>.
- Nguyen, B.T.; Lehmann, J.; Hockaday, W.C.; Joseph, S.; Masiello, C.A. Temperature sensitivity of black carbon decomposition and oxidation. *Environmental Science & Technology*, v.44, n.9, p.3324–3331, 2019. <https://doi.org/10.1021/es903016y>.
- Novotny, E.H.; Maia, C.M.B.F.; Carvalho, M.T.M.; Madari, B.E. Biochar: pyrogenic carbon for agricultural use - a critical review. *Revista Brasileira de Ciência do Solo*, v.39, n.2, p.321–344, 2015. <https://doi.org/10.1590/01000683rbcs20140818>.
- Oliveira, L.P. Síntese e caracterização de carvão vegetal ativado por meio de oxidação com HNO₃ e H₂O₂. *Macaíba: Universidade Federal do Rio Grande do Norte*, 2017. 41p. Undergraduate Thesis.
- Pandiarajan, A.; Kamaraj, R.; Vasudevan, S.; Vasudevan, S. OPAC (orange peel activated carbon) derived from waste orange peel for the adsorption of chlorophenoxyacetic acid herbicides from water: Adsorption isotherm, kinetic modelling and thermodynamic studies. *Bioresource Technology*, v.261, p.329–341, 2018. <https://doi.org/10.1016/j.biortech.2018.04.005>.
- Peng, X.; Ye, L.L.; Wang, C.H.; Zhou, H.; Sun, B. Temperature- and duration-dependent rice straw-derived biochar: characteristics and its effects on soil properties of an Ultisol in southern China. *Soil and Tillage Research*, v.112, n.2, p.159–166, 2011. <https://doi.org/10.1016/j.still.2011.01.002>.
- Robati, D.; Mirza, B.; Rajabi, M.; Moradi, O.; Tyagi, I.; Agarwal, S.; Gupta, V.K. Removal of hazardous Dyes-BR 12 and methyl orange using graphene oxide as an adsorbent from aqueous phase. *Chemical Engineering Journal*, v.284, p.687–697, 2016. <https://doi.org/10.1016/j.cej.2015.08.131>.
- Rodriguez, M.H.; Yperman, J.; Carleer, R.; Maggen, J.; Dadi, D.; Gryglewicz, G.; Van Der Bruggen, B.; Hernández, J.H.; Calvis, A.O. Adsorption of Ni(II) on spent coffee and coffee husk based activated carbon. *Journal of Environmental Chemical Engineering*, v.6, n.1, p.1161–1170, 2018. <https://doi.org/10.1016/j.jece.2017.12.045>.
- Santos, A.; Simões, R.; Tavares, M. Variation of some wood macroscopic properties along the stem of *Acacia melanoxylon* R. Br. adult trees in Portugal. *Forest Systems*, v.22, n.3, p.463–470, 2013. <https://doi.org/10.5424/fs/2013223-02421>.
- Silva, A.J.F.da; Moura, M.C. de P.A.; Santos, E. da S.; Pereira, J.E.S.; Barros Neto, E.L. de. Copper removal using carnauba straw powder: studies of equilibrium, kinetics and thermodynamics. *Journal of Environmental Chemical Engineering*, v.6, n.6, p.6828–6835, 2018. <https://doi.org/10.1016/j.jece.2018.10.028>.
- Spessato, L.; Bedin, K.C.; Cazetta, A.L.; Souza, I.P.A.F.; Duarte, V.A.; Crespo, L.H.S.; Silva, M.C.; Pontes, R.M.; Almeida, V.C. KOH-Super activated carbon from biomass waste: insights into the paracetamol adsorption mechanism and thermal regeneration cycles. *Journal of Hazardous Materials*, v.371, p.499–505, 2019. <https://doi.org/10.1016/j.jhazmat.2019.02.102>.
- Swiatkowski, A.; Pakula, M.; Biniak, S.; Walczyk, M. Influence of the surface chemistry of modified activated carbon on its electrochemical behaviour in the presence of lead(II) ions. *Carbon*, v.42, n.15, p.3057–3069, 2004. <https://doi.org/10.1016/j.carbon.2004.06.043>.
- Tiryaki, B.; Yagmur, E.; Banford, A.; Aktas, Z. Comparison of activated carbon produced from natural biomass and equivalent chemical compositions. *Journal of Analytical and Applied Pyrolysis*, v.105, p.276–283, 2014. <https://doi.org/10.1016/j.jaap.2013.11.014>.
- Trompowsky, P.M.; Benites, V. de M.; Madari, B.E.; Pimenta, A.S.; Hockaday, W.C.; Hatcher, P.G. Characterization of humic like substances obtained by chemical oxidation of eucalyptus charcoal. *Organic Geochemistry*, v.36, n.11, p.1480–1489, 2005. <https://doi.org/10.1016/j.orggeochem.2005.08.001>.
- Turčániová, L.; Škvarla, J.; Baláž, P.A. Contribution to the mechanism of formation of humic acids in coal. *Journal of Materials Synthesis and Processing*, v.8, n.5–6, p.359–363, 2000. <https://doi.org/10.1023/A:1011358831253>.
- Verheijen, F.; Jeffrey, S.; Bastos, A.C.; van der Velde, M.; Dias, I. Biochar application to soils: a critical review of effects on soil properties, processes and functions. *Ispra: European Commission*, 2010. 149p. <https://doi.org/10.2788/472>.
- Wang, B.; Lehmann, J.; Hanley, K. Hestrin, R.; Enders, A. Adsorption and desorption of ammonium by maple wood biochar as a function of oxidation and pH. *Chemosphere*, v.138, p.120–126, 2015. <https://doi.org/10.1016/j.chemosphere.2015.05.062>.
- Wang, Y.; Liu, R. H₂O₂ treatment enhanced the heavy metals removal by manure biochar in aqueous solutions. *Science of The Total Environment*, v.628–629, p.1139–1148, 2018. <https://doi.org/10.1016/j.scitotenv.2018.02.137>.
- Xu, Z.; Xu, X.; Tsang, D.C.W.; Cao, X. Contrasting impacts of pre- and post-application aging of biochar on the immobilization of Cd in contaminated soils. *Environmental Pollution*, v.242, Part B, p.1362–1370, 2018. <https://doi.org/10.1016/j.envpol.2018.08.012>.
- Yang, J.; Yu, M.; Chen, W. Adsorption of hexavalent chromium from aqueous solution by activated carbon prepared from longan seed: kinetics, equilibrium and thermodynamics. *Journal of Industrial and Engineering Chemistry*, v.21, p.414–422, 2015. <https://doi.org/10.1016/j.jiec.2014.02.054>.
- Yao, S.; Zhang, J.; Shen, D.; Xiao, R.; Gu, S.; Zhao, M.; Liang, J. Removal of Pb(II) from water by the activated carbon modified by nitric acid under microwave heating. *Journal of Colloid and Interface Science*, v.463, p.118–127, 2016. <https://doi.org/10.1016/j.jcis.2015.10.047>.

Zhang, K.; Sun, P.; Faye, M.C.A.S.; Zhang, Y. Characterization of biochar derived from rice husks and its potential in chlorobenzene degradation. *Carbon*, v.130, p.730-740, 2018. <https://doi.org/10.1016/j.carbon.2018.01.036>.

Zuo, X.; Liu, Z.; Chen, M. Effect of H₂O₂ concentrations on copper removal using the modified hydrothermal biochar. *Bioresource Technology*, v.207, p.262-267, 2016. <https://doi.org/10.1016/j.biortech.2016.02.032>.